

Figure 1. Effect of catalyst concentration on rate of reaction (1) using data of Table I. Catalysts are: (A) TBAB; (B) NMI; (C) TBAB + NMI, equimolar, calculated assuming additivity of A and B; (D) TBAB + NMI, equimolar, found.

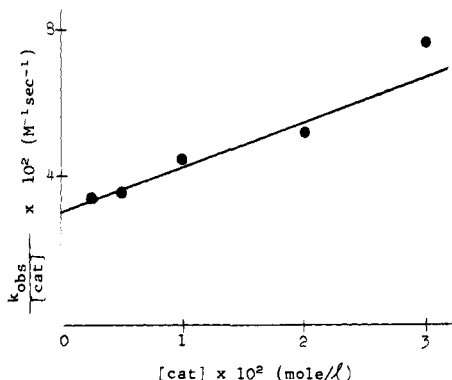


Figure 2. Plot of $k_{\text{obsd}}/[\text{cat}]$ vs. $[\text{cat}]$ for data of curve D, Figure 1.

tion (k_{cocat}) would be predicted to be very large, but at low catalyst levels its contribution to the overall process would be severely mediated by its bimolecular nature. To obtain definitive information on the extent of this cocatalysis we undertook a kinetic study of the formation of Ib utilizing the more water soluble nucleophile, sodium 2-(6-chloropyridinolite).

The observed pseudo-first-order rate constants (k_{obsd}) are summarized in Table I for the uncatalyzed, NMI or TBAB catalyzed, and cocatalyzed reactions.⁷ The dependence of k_{obsd} on catalyst concentration is shown in Figure 1. Individually, the rate constants for both the phase transfer (curve A) and amine (curve B) catalyzed reaction give the expected first-order behavior. However, k_{obsd} for the combined catalysts (curve D) fits the calculated, additive curve C only at low concentrations, the sharply upward deviation at concentrations greater than 0.01 M indicating the presence of an additional, higher order component in k_{obsd} .

The overall rate (neglecting an insignificant contribution from the uncatalyzed reaction) for the binary catalysis process may be written as shown in eq 4 and 5.

$$\frac{-d(\text{DMPCT})}{dt} = k_{\text{PTC}}[\text{TBAB}][\text{DMPCT}] + k_{\text{Nu}}[\text{NMI}][\text{DMPCT}] + k_{\text{cocat}}[\text{TBAB}][\text{NMI}][\text{DMPCT}] \quad (4)$$

and

$$k_{\text{obsd}} = k_{\text{PTC}}[\text{TBAB}] + k_{\text{Nu}}[\text{NMI}] + k_{\text{cocat}}[\text{TBAB}][\text{NMI}] \quad (5)$$

From these rate equations and the data of Table I, all the pertinent rate constants may be evaluated. For equivalent concentrations of the two catalysts the data may be plotted

as in Figure 2, the slope yielding $k_{\text{cocat}} = 1.3 \pm 0.3 \text{ l}^2 \text{ mol}^{-2} \text{ s}^{-1}$ and the intercept = $k_{\text{PTC}} + k_{\text{Nu}} = 3 \times 10^{-2} \text{ l} \cdot \text{mol}^{-1} \text{ s}^{-1}$. Plots of $[\text{TBAB}]$ vs. k_{obsd} for three different NMI concentrations and of $[\text{NMI}]$ vs. k_{obsd} for differing $[\text{TBAB}]$ give straight lines whose slopes increase with increasing $[\text{NMI}]$ in the former and $[\text{TBAB}]$ in the latter. This result requires that the overall catalytic effect of one catalyst is increased in proportion to the concentration of the other; i.e., a cocatalytic effect has been demonstrated.

From the slopes and intercepts of k_{obsd} vs. $[\text{cat}]$ for non-equivalent catalyst concentrations, additional rate data may be obtained⁸ which agree well with each other but differ somewhat from those evaluated from Figure 2. The average ($\pm 10\%$) values, calculated as pseudo-first-order rate constants for 1.0 M catalysts are: $k_{\text{PTC}} = 45$, $k_{\text{Nu}} = 290$, and $k_{\text{cocat}} = 8500 \text{ s}^{-1}$. Using these k 's we calculate that at the 0.02 M catalyst level, 33% of the total reaction proceeds via eq 3.

Finally, we can again demonstrate that the optimum features of the individual catalysts are incorporated in cocatalysis: using equivalent amounts of 0.2 M pyridinolite and DMPCT with 0.02 M catalysts the rate of the cocatalyzed process is 1.5 times that of the sum of the individually catalyzed reactions while still maintaining the PTC-catalyzed selectivity ratio of 9:1 (ester:hydrolysis) rather than the NMI-catalyzed selectivity of 1:1. The full implication of these results, particularly for bioorganic applications, remains to be explored.⁹

Acknowledgment. The authors are grateful to D. E. Golan and R. A. Dubois for experimental contributions and to Professors W. P. Jencks and C. P. Lillya for critical discussions.

References and Notes

- Reviews: J. R. Cox and O. B. Ramsay, *Chem. Rev.*, **64**, 317 (1964); W. P. Jencks, "Catalysis in Chemistry and Enzymology", McGraw-Hill, New York, N.Y., 1969, Chapter 2; M. L. Bender, "Mechanisms of Homogeneous Catalysis from Protons to Proteins", Wiley Interscience, New York, N.Y., 1971.
- Reviews: J. Dockx, *Synthesis*, 441 (1973); E. V. Dehmow, *Angew. Chem., Int. Ed. Engl.*, **13**, 170 (1974).
- The disappearance of DMPCT and the formation of I were monitored by GLC analysis of the organic layer, using an internal standard for quantification.
- F. Cramer and H. Schaller, *Chem. Ber.*, **94**, 1634 (1961); T. Wagner-Jauregg and B. E. Hackley Jr., *J. Am. Chem. Soc.*, **75**, 2125 (1953).
- F. M. Menger, *J. Am. Chem. Soc.*, **92**, 5965 (1970).
- C. M. Starks and R. M. Owens, *J. Am. Chem. Soc.*, **95**, 3613 (1973); H. H. Freedman and R. A. Dubois, *Tetrahedron Lett.*, 3251 (1975).
- Standard conditions: equal volumes of aqueous 0.8 M sodium 2-(6-chloropyridinolite) and 0.2 M DMPCT in CH_2Cl_2 , 25°, stirred at 500 rpm. Rate constants were determined from first-order plots of DMPCT disappearance and were independent of pyridinolite concentration under our conditions.
- For details of an analogous kinetic treatment see W. P. Jencks and M. Gilchrist, *J. Am. Chem. Soc.*, **88**, 104 (1966).
- Preliminary results with carboxylic acid chlorides and anhydrides have demonstrated the marked advantage of PTC, but not of cocatalysis, for phenolate acylations in biphasic media.

R. W. Ridgway, H. S. Greenside, H. H. Freedman*

Dow Chemical U.S.A.
Central Research—New England Laboratory
Wayland, Massachusetts 01778

Received December 12, 1975

Electrochemical Synthesis and Structural Characterization of the Iron-Sulfur Cluster Cation¹

$[(\eta\text{-C}_5\text{H}_5)_2\text{Fe}_2(\text{S}_2)(\text{SC}_2\text{H}_5)_2]^+$

Sir:

The synthesis and structural analysis² of $[\text{Cp}_2\text{Fe}_2(\text{S}_2)(\text{SC}_2\text{H}_5)_2]$ (1) ($\text{Cp} = \eta\text{-C}_5\text{H}_5$) have expanded the growing list of crystallographically determined mole-

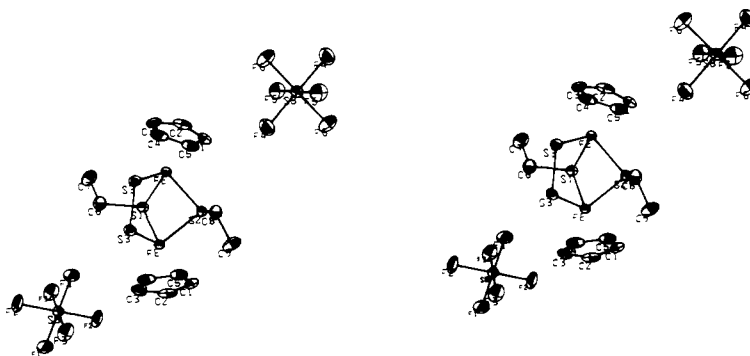
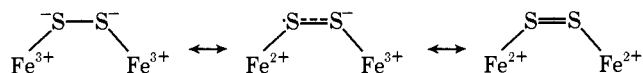


Figure 1. Stereoscopic view of the structure of $[\text{Cp}_2\text{Fe}_2(\text{S}_2)(\text{SC}_2\text{H}_5)_2]^+\text{SbF}_6^-$. The two independent octahedral sets of half-weighted fluorine atomic positions are shown in positions which do not make close contact with the methyl carbons of the ethyl mercaptan bridges.

cles containing the S_2 ligand.³⁻⁸ A planar $\text{M}_2\text{-S}_2$ configuration was found in **1** which was not previously observed in any cluster compound. The unique iron-sulfur core of this complex has been proposed^{2,9} as a possible model candidate for the active site of iron-labile sulfur proteins. The mode of bonding within the iron-sulfur core of this compound has not been well understood, however, possibly due to its unique stereochemical configuration. If the usual electron counting processes are applied (e.g., S_2^{2-} is a four-electron donor) and the conspicuous absence of a direct electron pair metal-metal bond is taken into account, each iron atom in the cluster would be one electron short of the required noble-gas configuration.

The seemingly contradictory observation that **1** is essentially diamagnetic at room temperature was ascribed to strong magnetic coupling between iron centers via the bridging ligands, which can be looked upon as equivalent to electron delocalization through the resonance forms:²



However, subsequent magnetic susceptibility measurements over the temperature range 4–300 K failed to provide evidence for the above described behavior, and consequently it became necessary to investigate the redox properties of **1** as a means of obtaining further bonding information.¹⁰ The structural characterization of both components of an electrochemically reversible couple in cluster compounds^{11,12} has demonstrated the power of this technique to yield information regarding bonding properties and, in particular, the nature of the highest occupied molecular orbital.¹³ We now wish to report the successful application of such a characterization toward the derivation of what we believe to be a unique electron-pair coupling mechanism which is consistent with the observed structural and magnetic properties but requires neither a superexchange mechanism to couple unpaired spins through bridging ligands nor the absence of strong metal-metal interaction.

Two new cluster products have been isolated during the course of the electrochemical study of **1**.¹⁰ The first of these, **2**, the product of a reversible one-electron oxidation, is the monocation of the disulfide bridged dimer; its structure determined as both PF_6^- and SbF_6^- salts is presented here. The structure of a dicationic compound, $[\text{CpFe}(\text{NCCH}_3)(\text{SC}_2\text{H}_5)_2]^{2+}$, obtained from a further non-reversible one-electron oxidation of the monocation has been structurally characterized and will be reported elsewhere.¹⁴

The x-ray data were collected and analyzed as in previous structures reported from this laboratory.¹⁵ The PF_6^- salt of the monocation, $[\text{Cp}_2\text{Fe}_2(\text{SC}_2\text{H}_5)_2]^+$, crystallized in the monoclinic space group $P2_1/m$ (or its noncentric ana-

Table II. Some Important Interatomic Distances and Angles for $[\text{Cp}_2\text{Fe}_2(\text{S}_2)(\text{SEt})_2]^n$ ($n = 0, +1$)^a

	$[\text{Cp}_2\text{Fe}_2(\text{S}_2)(\text{SEt})_2]^b$	$[\text{Cp}_2\text{Fe}_2(\text{S}_2)(\text{SEt})_2]^+$
Fe-Fe	3.307 (1)	3.059 (1)
Fe-S _s	2.129 (2)	2.135 (1)
Fe-S _{Et}	2.281 (2)	2.250 (1)
S-S	2.023 (3)	1.987 (1)
S _{Et} -S _{Et}	2.823	3.038
S _s -S _{Et}	3.226 (1)	3.263 (1)
Fe-S-Fe	107.55° (7)	104.54° (2)
Fe-S _{Et} -Fe	92.95° (5)	85.66° (4)

^a In angstroms and degrees; standard deviations in parentheses refer to the least significant digit; Et = C_2H_5 . ^b Taken from ref 2.

logue $P2_1$) with cell parameters of $a = 6.711$ (3) Å, $b = 19.57$ (9) Å, $c = 7.87$ (4) Å, $\beta = 91.2$ (4)° ($d_{\text{calcd}} = 1.75$, $d_{\text{measd}} = 1.8$). The iron, sulfur, Cp ring carbons, and P positions were determined in the centric group. Early in the structure determination disorder problems became apparent in both the ethyl carbon and fluorine atomic positions. The unweighted R factor at this point was 18%. Better quality crystals became available at this stage of the refinement in the form of the SbF_6^- salt which is isostructural: $a = 6.777$ (3) Å, $b = 19.849$ (7) Å, $c = 7.909$ (3) Å, $\beta = 91.56$ (3)°. Disorder problems involving both the ethyl carbon and fluorine atomic positions were found to occur in this salt form as well. Close examination of the structure revealed that these problems were related, and a structural model was determined which allowed a successful refinement in the centric space group; the model included (1) the placement of two independent octahedral sets of fluorine atoms about the Sb atom and (2) the disorder of the methyl carbon atoms across a crystallographic mirror plane which bisects the Fe-Fe vector and contains the sulfur atoms of the bridging mercapto groups. Further structural refinement was carried out for only the SbF_6^- salt. An anisotropic, full-matrix, least-squares refinement based on 2854 absorption-corrected data with $|F| > 4\sigma(F)$ yielded an unweighted R_1 value of 3.3%. Along with the two independent octahedral sets of half-weighted fluorine atoms and half-weighted methyl carbons, idealized hydrogen atomic positions for the cyclopentadienyl group and methylene carbons, which were computed after each least-squares cycle,¹⁶ were included in the refinement. The hydrogen positional and isotropic thermal parameters were not allowed to vary. A listing of atomic positional parameters will appear in Table I in the microfilm edition of this volume of the journal.

The x-ray evidence, along with the analytical data,¹⁰ definitely establishes this compound to be the hexafluoroantimonate (or hexafluorophosphate) salt of the monocation $[\text{Cp}_2\text{Fe}_2(\text{S}_2)(\text{SC}_2\text{H}_5)_2]^+$ (Figure 1). Important structural

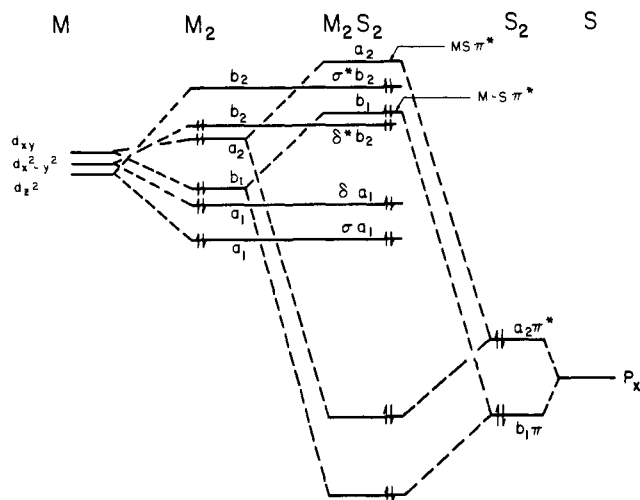


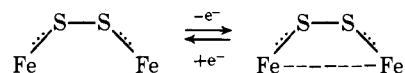
Figure 2. Proposed qualitative molecular orbital energy scheme for the Fe_2S_2 interaction in $[\text{Cp}_2\text{Fe}_2(\text{S}_2)(\text{SC}_2\text{H}_5)_2]^n$ ($n = 0, +1$).

parameters for the SbF_6^- salt of the monocation **2** are given in Table II, along with those of the parent neutral dimer for comparison purposes. The structure of the iron-sulfur core in the monocation **2** is similar to that in the neutral parent **1**. The unique planarity of the Fe-S-S-Fe bridge is retained upon oxidation and is in fact crystallographically imposed by the mirror plane passing through S(1) and S(2). The most salient difference between the two is a dramatic decrease of 0.248 Å in the Fe-Fe distance from a value of 3.307 (1) Å in the neutral species to 3.059 (1) Å in the monocation, well within the range expected for a one-electron iron-iron interaction.¹¹

In addition to the observation that compound **1** does not follow normal electron counting rules, the results presented here include several structural facts which would have to be explained by any bonding model proposed for the system. The S-S and iron-sulfur bonding distances are practically unaffected by removal of an electron from the neutral dimer; yet the Fe-Fe distance decreases by an amount consistent with the formation of a one-electron metal-metal bond. The average iron-sulfur ($\mu_2\text{-S}_2$) distance of 2.13 Å for the bridging disulfide ligand is approximately 0.1 Å shorter than that expected from an examination of comparable M-S ($M = \text{Co}, \text{Fe}$) bond lengths in other cluster compounds containing disulfide ligands.⁴⁻⁸

The development of a qualitative bonding scheme for transition metal cluster compounds usually assumes the metal-ligand interactions to be energetically well-separated from metal-metal interactions. This results in a group of highest filled molecular orbitals which are primarily metal in character. Filling these orbitals with available electrons would lead to the prediction of a metal-metal bond for the neutral dimer which is not observed. A suitable perturbation on this model which accounts for all of the observed structural characteristics in this molecule will be described below. For convenience, the local Cartesian coordinate systems for the iron and sulfur atoms were chosen such that the z axis was oriented toward the molecular twofold axis and perpendicular to it, while the y axis lies parallel to it. When the metal-ligand and ligand-ligand σ bonding interactions are accounted for, there remain six primarily metal orbitals (which can be visualized as arising from the d_{z^2} , $d_{x^2-y^2}$, and d_{xy} atomic orbitals on each of the irons) which are shown under M_2 in Figure 2. When the orbitals are filled with the remaining valence electrons this model predicts a metal-metal bond; the lowest unoccupied molecular orbital would be expected to be a metal-metal σ^* orbital. A

mixing of essentially nonbonding M_2 and S_2 orbitals to form a bonding interaction of a π -type orbital of the S_2 ligand with the appropriate iron $3d\pi$ orbitals (shown under M_2S_2 in Figure 2) would be expected to increase the Fe-S bond order, account for the planarity of the Fe_2S_2 system, and at the same time result in the highest occupied molecular orbital being primarily an iron-iron antibonding orbital. Removal of an electron from this highest energy orbital would result in a net bonding interaction between the metals in accord with the observed decrease in metal-metal distance. This can be illustrated schematically as follows:



Further oxidation of the monocation to a dication would be expected to manifest itself in a further shortening of the Fe-Fe distance to that expected for an electron-pair metal-metal bond. However, this would presumably place considerable angular strain on the Fe_2S_2 fragment in harmony with the observed loss of the S_2 ligand to form the solvent-ligated dicationic species^{10,14} at ambient temperatures. The energy separation of the highest occupied and lowest unoccupied molecular orbitals is expected to be sufficient to prevent the observation of anomalous temperature dependent magnetic properties associated with an electron pair coupling via a weak superexchange mechanism. Under these conditions, where the S_2 forms a planar bridge between the irons, the disulfide ligand can formally be considered as donating six electrons into the diiron set rather than the expected four electrons.

Studies directed toward low temperature isolation and structural characterization of the disulfur containing dication are in progress and should help to clarify the structure and bonding in the disulfide dimer and its derivatives.

Supplementary Material Available: A listing of atomic positional parameters (Table I) (2 pages). Ordering information is given on any current masthead page.

References and Notes

- (1) This work was performed under the auspices of the U.S. Energy Research and Development Administration.
- (2) (a) G. J. Kubas, T. G. Spiro, and A. Terzis, *J. Am. Chem. Soc.*, **95**, 273 (1973); (b) A. Terzis and R. Rivest, *Inorg. Chem.*, **12**, 2132 (1973).
- (3) W. D. Bonds, Jr. and J. A. Ibers, *J. Am. Chem. Soc.*, **94**, 3413 (1972).
- (4) D. L. Stevenson, V. R. Magnuson, and L. F. Dahl, *J. Am. Chem. Soc.*, **89**, 3727 (1967).
- (5) C. H. Wei and L. F. Dahl, *Inorg. Chem.*, **4**, 1 (1965).
- (6) V. A. Uchtman and L. F. Dahl, *J. Am. Chem. Soc.*, **91**, 3756 (1969).
- (7) P. J. Vergamini, R. R. Ryan, and G. J. Kubas, Abstracts, Meeting of the American Crystallographic Association, Gainesville, Fla. Jan 14-18, 1973, No. D12.
- (8) P. J. Vergamini, R. R. Ryan, and G. J. Kubas, in preparation for publication.
- (9) W. H. Orme-Johnson, *Annu. Rev. Biochem.*, 159 (1973).
- (10) G. J. Kubas, P. J. Vergamini, M. P. Eastman, and K. B. Prater, submitted for publication.
- (11) N. G. Connelly and L. F. Dahl, *J. Am. Chem. Soc.*, **92**, 7472 (1970).
- (12) G. L. Simon and L. F. Dahl, *J. Am. Chem. Soc.*, **95**, 2164 (1973).
- (13) B. K. Teo, M. B. Hall, R. F. Fenske, and L. F. Dahl, *J. Organomet. Chem.*, **70**, 413 (1974).
- (14) P. J. Vergamini, R. R. Ryan, and G. J. Kubas, submitted for publication.
- (15) B. I. Swanson and R. R. Ryan, *Inorg. Chem.*, **12**, 283 (1973), for example.
- (16) J. Calabrese, MIRAGE. A General Vector Program for Obtaining Atomic Coordinates, Ph.D. Thesis (Appendix III), University of Wisconsin, Madison, Wisc., 1971.
- (17) It should be emphasized that the low symmetry of the complex allows considerable mixing of the orbitals beyond the interactions illustrated. We have delineated only the features of the scheme we believe to be essential to account for the physical observations.

P. J. Vergamini,* R. R. Ryan, G. J. Kubas
The University of California
Los Alamos Scientific Laboratory
Los Alamos, New Mexico 87545
Received March 21, 1975